DOI: 10.1002/chem.200501238

Synthesis of Fullerodendrons with an Ammonium Unit at the Focal Point and Their Cooperative Self-Assembly on a Fluorescent Ditopic Crown Ether Receptor

Jean-François Nierengarten,*[a] Uwe Hahn,[a] Ali Trabolsi,[b] Haiko Herschbach,[c]
François Cardinali,[a] Mourad Elhabiri,[b] Emmanuelle Leize,[c]
Alain Van Dorsselaer,*[c] and Anne-Marie Albrecht-Gary*[b]

Abstract: Dendritic branches with 1, 2, or 4 peripheral fullerene subunits and an ammonium function at the focal point have been prepared. Their ability to form self-assembled dendritic structures with oligophenylenevinylene receptors bearing one or two crown ether moieties has been evidenced by ES-MS studies for the first time. These supramolecular complexes are multicomponent photoactive devices in which the emission of the central receptor is dramatically quenched by the fullerene units. This new property resulting from the association of the different molecular subunits allowed detailed investigations of the self-assembly process by means of fluorescence titrations. The binding studies have revealed positive cooperative effects for the assembly of the fullerodendrimers with the ditopic receptor. Interestingly, the stability of the supramolecular 2:1 structures increases as the size of the dendritic unit increases. This positive dendritic effect has been explained by the larger number of possible intramolecular fullerene–fullerene interactions between the two dendritic guests when the number of fullerene subunits is increased.

Keywords: cooperative phenomena · crown compounds · dendrimers · fullerenes · supramolecular chemistry

Introduction

Because of their inherent branched structure, dendrimers are intrinsic scaffolds for the preparation of high-molecular-weight compounds.[1] One of the most appealing features of dendritic derivatives is the possibility of tuning their properties by changing the number, chemical nature, and relative position of functional units within the branched structure.[1] In this way, dendritic architectures are capable of generating specific properties.[1] However, the preparation of large dendrimers remains quite difficult and often involves a high number of synthetic steps thus limiting their accessibility. The self-assembly of dendritic macromolecules on the basis of noncovalent interactions[2] is an interesting alternative because the synthesis is itself restricted to the preparation of small dendritic building blocks, and self-aggregation leads to the dendrimer thus avoiding tedious final synthetic steps with highly crowded precursors. Different strategies have been developed for the self-assembly of dendritic architectures.[2] The first one is to prepare dendrons with a core unit that is capable of recognizing itself[3] or a polytopic receptor,[4] thus leading to the formation of a dendrimer. The

---

[a] Dr. J.-F. Nierengarten, Dr. U. Hahn, Dr. F. Cardinali
Groupe de Chimie des Fullerènes et des Systèmes Conjugués
Laboratoire de Chimie de Coordination du CNRS
205 route de Narbonne, 31077 Toulouse Cedex 4 (France)
Fax: (+33) 5-6155-3003
E-mail: jfnierengarten@lcc-toulouse.fr

[b] A. Trabolsi, Dr. M. Elhabiri, Dr. A.-M. Albrecht-Gary
Laboratoire de Physico-Chimie Bioinorganique
Université Louis Pasteur et CNRS (UMR 7509)
Ecole Européenne de Chimie, Polymères et Matériaux (ECPM)
25 rue Becquerel, 67200 Strasbourg (France)
Fax : (+33) 3-9024-2639
E-mail: amalbre@chimie.u-strasbg.fr

[c] H. Herschbach, Dr. E. Leize, Dr. A. Van Dorsselaer
Laboratoire de Spectrométrie de Masse Bio-organique
Ecole Européenne de Chimie, Polymères et Matériaux (ECPM)
Université Louis Pasteur et CNRS
25 rue Becquerel, 67087 Strasbourg Cedex 2 (France)
Fax : (+33) 3-9024-2781
E-mail: vandors@chimie.u-strasbg.fr

Supporting information for this article is available on the WWW under http://www.chemeurj.org/ or from the author.

second one is to noncovalently assemble layers or generations via recognition units on the periphery or on the branched monomers inside the dendrimer.[5] As part of this research, we have recently shown that the noncovalent approach is particularly well suited for the preparation of fullerene-rich dendrimers.[6] In particular, we have prepared supramolecular dendrimers resulting from the dimerization of fullerene-functionalized dendrons by a quadruple hydrogen-bonding motif.[6b] Having shown that the construction of dendrimers containing multiple C_{60} subunits by noncovalent interactions is successful, the next challenges include a comprehensive investigation of the self-assembly of such large supermolecules and the preparation of fullerene-rich nanostructures with new properties. In this paper, we report the self-assembly of fullerene-functionalized dendritic branches bearing an ammonium function at the focal point on a fluorescent ditopic crown ether receptor. The resulting 2:1 supramolecular complexes are multicomponent photoactive devices in which the emission of the central ditopic receptor is dramatically quenched by the peripheral fullerene units. This new property, which results from the association of the different molecular subunits, allowed detailed investigations of the self-assembly process. Interestingly, positive cooperative effects have been evidenced and the stability of the supramolecular 2:1 structures increases as the size of the dendritic scaffold increases. This positive dendritic effect has been explained by the larger number of possible intramolecular interactions between the two dendritic guests when their structure becomes larger.

Results and Discussion

Synthesis: We recently described the assembly of the C_{60}-ammonium cation **G1NH$_3^+$** with the oligophenylenevinylene (OPV) derivatives **1** and **2** (Figure 1). Interestingly, the receptor bearing two crown ether moieties led to the cooperative self-assembly of the 2:1 complex as a result of intramolecular fullerene–fullerene interactions.[7] This prompted us to increase the number of C_{60} units attached to the ammonium building block in order to generate additional possible intramolecular interactions between the two guests in the 2:1 assembly. In this way, the stability of the supramolecular ensembles could be increased. With this idea in mind, fullerodendrimers **G2NH$_3^+$** and **G3NH$_3^+$** were designed (Figure 1).

The synthesis of **G2NH$_3^+$** and **G3NH$_3^+$** is depicted in Scheme 1. Precursors **3** and **4** were prepared as previously reported.[8] Reaction of **3** with alcohol **5**[9] under esterification conditions [*N*,*N'*-dicyclohexylcarbodiimide (DCC), 1-hydroxy-benzotriazole (HOBt), and 4-dimethylaminopyridine (DMAP)] afforded the *t*-butyloxycarbonyl (Boc)-protected dendron **G2NHBoc** of the second generation in 89% yield. Subsequent treatment with CF_3CO_2H in CH_2Cl_2 gave

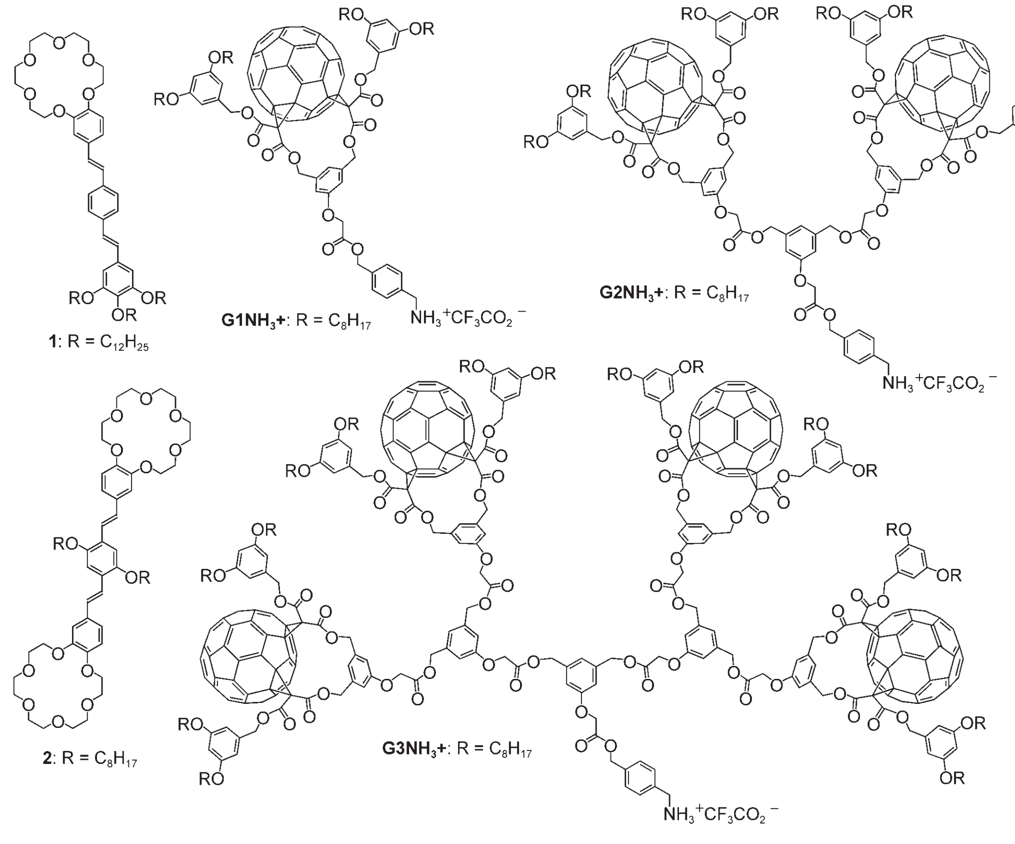

Figure 1. Fullerodendrons **G(1–3)NH$_3^+$** and crown ether receptors **1** and **2**.

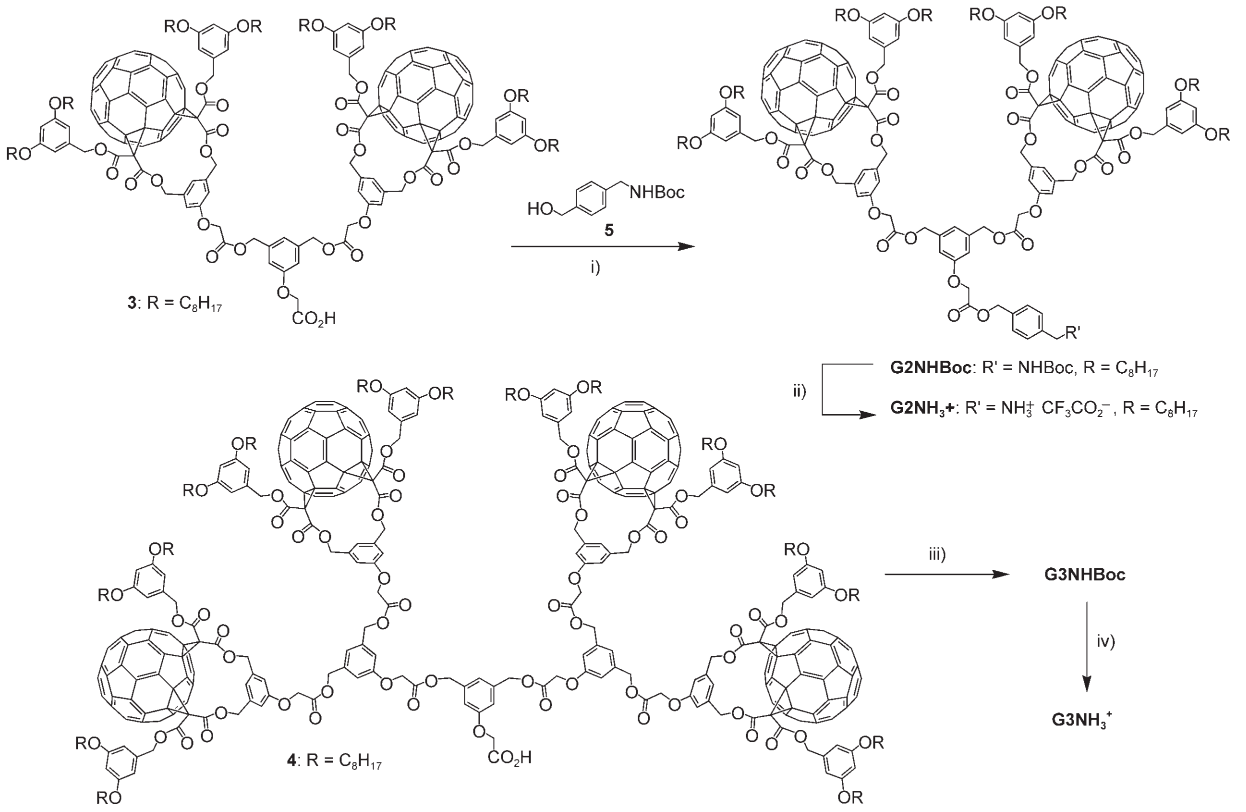

Scheme 1. Reagents and conditions: i) DCC, HOBt, DMAP, CH_2Cl_2, 0 to 25 °C (89 %); ii) CF_3CO_2H, CH_2Cl_2, 25 °C (79 %); iii) **5**, DCC, HOBt, DMAP, CH_2Cl_2, 0 to 25 °C (67 %); iv) CF_3CO_2H, CH_2Cl_2, 25 °C (63 %).

$G2NH_3^+$ as its trifluoroacetate salt in 79 % yield. The third-generation derivative **$G3NH_3^+$** was prepared from **4** by repeating the same reaction sequence. Esterification with alcohol **5** (DCC, HOBt, DMAP) and deprotection of the resulting **G3NHBoc** by treatment with CF_3CO_2H gave **$G3NH_3^+$**.

Owing to the presence of the four long alkyl chains on each peripheral fullerene unit, compounds **G2NHBoc**/**G3NHBoc** and **$G2NH_3^+$**/**$G3NH_3^+$** have good solubility in common organic solvents, such as toluene, CH_2Cl_2, $CHCl_3$, or THF, and complete spectroscopic characterization was easily achieved. The structure of both **$G2NH_3^+$** and **$G3NH_3^+$** was further confirmed by using mass spectrometry. The expected molecular ion peak was observed at m/z = 3884 for **$G2NH_3^+$** (calcd for $C_{262}H_{194}NO_{33}$: 3884.34 $[M{-}CF_3COO^-]^+$) and m/z = 7825 for **$G3NH_3^+$** (calcd for $C_{526}H_{386}NO_{69}$: 7824.68 $[M{-}CF_3COO^-]^+$).

Mass spectrometry: The supramolecular complexes obtained from the fullerene-containing dendrons **$G(1–3)NH_3^+$** and the crown ether receptors **1** and **2** were first characterized in the gas phase by electrospray mass spectrometry (ES-MS). Unlike other mass spectrometric methods, ES-MS allows pre-existing ions in solution to be transferred to the gas phase without fragmentation[10] and thus appeared to be ideally suited to characterize the noncovalent complexes formed from **$G(1–3)NH_3^+$** and **1** or **2**.[11] The positive ES mass spectrum recorded under mild conditions (extracting cone voltage V_c = 200 V) from a 1:1 mixture of **1** and **$G2NH_3^+$** displayed a singly charged ion peak at m/z = 4953.9, which can be assigned to the 1:1 complex [**$G2NH_3^+$ ·1**] after loss of the trifluoroacetate counteranion (calculated m/z: 4953.92). Under harsher experimental conditions (V_c = 400 V, Figure 2), the spectrum was still dominated by the signal at m/z = 4953.9, but a singly charged ion peak attributed to the nonassociated dendritic cationic moiety of **$G2NH_3^+$** was also observed at m/z = 3884.0 (calculated $m/$

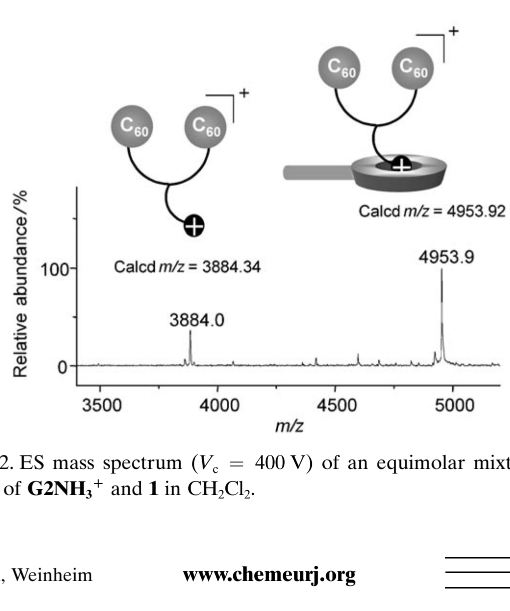

Figure 2. ES mass spectrum (V_c = 400 V) of an equimolar mixture (2×10^{-5} M) of **$G2NH_3^+$** and **1** in CH_2Cl_2.

z: 3884.34). It is worth noting that the intensity of the latter signal was increased as the V_c value was increased, thus the peak corresponding to **G2NH$_3$$^+$** mainly originated from the fragmentation of the 1:1 supramolecular complex [**G2NH$_3$$^+$ ·1**] initially present in solution.

As shown in Figure 3, the positive ES mass spectra obtained at low V_c value (200 V) from a 2:1 mixture of **G2NH$_3$$^+$** and **2** was dominated by the doubly charged ion peak at m/z = 4387.8 which can be assigned to the 2:1 complex [(**G2NH$_3$$^+$**)$_2$·**2**] after loss of the two trifluoroacetate counteranions (calculated m/z: 4387.99). The ion peaks corresponding to the 1:1 ensemble [**G2NH$_3$$^+$·2**] and to the non-associated dendritic cationic moiety of **G2NH$_3$$^+$** were also detected but their intensity was very low suggesting that fragmentation was quite limited under these experimental conditions.

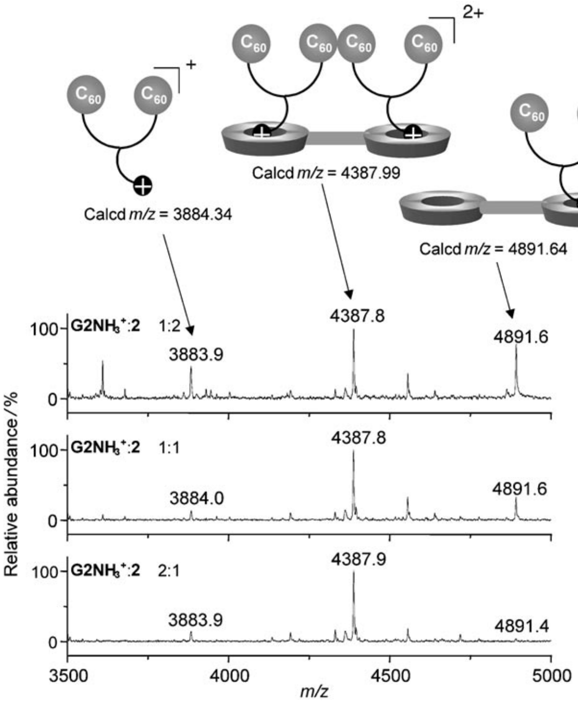

Figure 3. ES mass spectra (V_c = 200 V) of 1:2 (top), 1:1 (center), and 2:1 (bottom) mixtures (2×10^{-5} M) of **G2NH$_3$$^+$** and **2** in CH$_2Cl_2$.

Interestingly, the spectra recorded under similar conditions (V_c = 200 V) from 1:1 and 1:2 mixtures of **G2NH$_3$$^+$** and **2** were still dominated by the signal ascribed to the 2:1 complex [(**G2NH$_3$$^+$**)$_2$·**2**]. As the fragmentation level is quite low under these experimental conditions, the self-assembled array [(**G2NH$_3$$^+$**)$_2$·**2**] must be the most abundant species in all the analyzed solutions. The latter observation strongly suggests an increased stability of the 2:1 complex [(**G2NH$_3$$^+$**)$_2$·**2**] and is in perfect agreement with the positive cooperative effect deduced from the absorption and emission binding studies (see below). The stability of the 2:1 supramolecular array obtained from **G2NH$_3$$^+$** and **2** was also deduced from the ES mass spectra recorded under harsher conditions. This is shown in Figure 4 for the spectra obtained from the 1:1 mixture of **G2NH$_3$$^+$** and **2** at different V_c values ranging from 200 to 400 V. Under the harshest conditions (V_c = 400 V), the spectrum was no longer dominated by the doubly charged ion peak at m/z = 4387.8; however, the intensity of this signal was still quite high. In all the spectra, the diagnostic peaks of the 1:1 complex [**G2NH$_3$$^+$·2**] and the uncomplexed **G2NH$_3$$^+$** were also detected. Their intensity relative to the peak of the 2:1 complex was clearly increased when the V_c value was increased as a result of the fragmentation of [(**G2NH$_3$$^+$**)$_2$·**2**], which was initially present in solution. Finally, it can also be noted that characteristic fragments[12] were present in all spectra. In particular, cleavage of one 3,5-dioctyloxybenzylic ester unit in **G2NH$_3$$^+$**, with or without subsequent decarboxylation, was always observed and led to signals at [$M-(C_{23}H_{39}O_2)$] and [$M-(C_{24}H_{39}O_4)$].

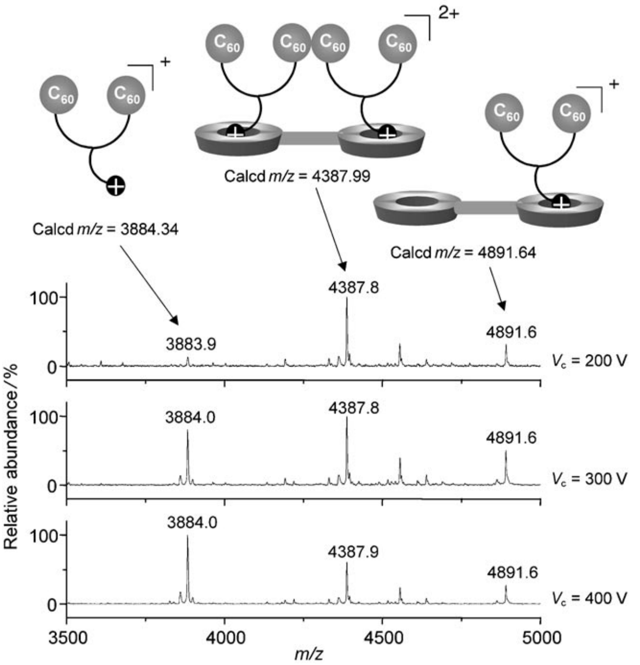

Figure 4. ES mass spectra recorded at different V_c values of a 1:1 mixture (2×10^{-5} M) of **G2NH$_3$$^+$** and **2** in CH$_2Cl_2$ (top: V_c = 200 V, center: V_c = 300 V; bottom: V_c = 400 V).

The ES mass spectrometric studies of mixtures of **G1NH$_3$$^+$** and **1** or **2** gave results similar to those described above for the second-generation ammonium derivative **G2NH$_3$$^+$**. In contrast, the analysis of the supramolecular complexes resulting from the association of **G3NH$_3$$^+$** with **1** and **2** was found to be more difficult. Indeed, the response factor was decreased when the molecular weight was increased and it was only possible to detect ion peaks for the largest compounds at high V_c values. Under these experimental conditions, the relative intensity of the different signals was no longer significant owing to the high level of fragmentation of the ammonium–crown ether complexes, as seen in the ES-MS studies of the first- and second-generation complexes. The positive ES mass spectrum of an equimolar mixture of **1** and **$G3NH_3^+$** (V_c = 350 V, Figure 5) displayed two singly charged ion peaks at m/z = 7824.6 and 8893.9 that can be assigned to the cationic moieties of **$G3NH_3^+$** (calculated m/z: 7824.68) and [**$G3NH_3^+$·1**] (calculated m/z: 8894.26), respectively.

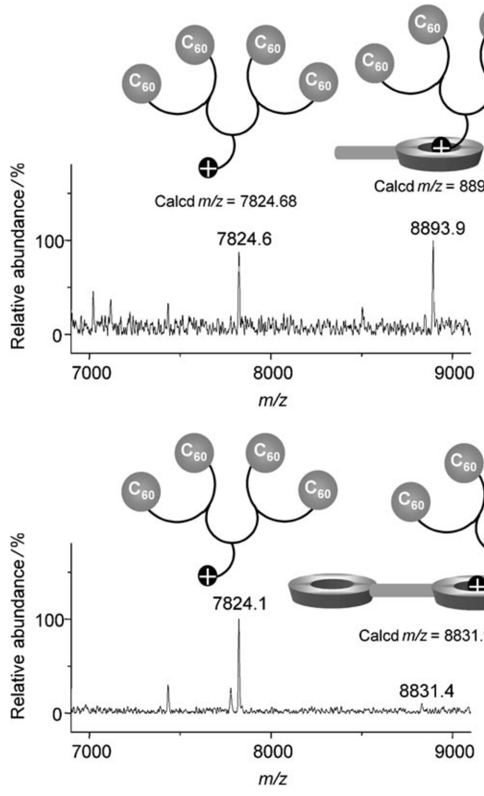

Figure 5. ES mass spectra (V_c = 350 V) of a 1:1 mixture (2×10^{-5} M) of **$G3NH_3^+$** and **1** in CH_2Cl_2 (top) and of a 2:1 mixture (2×10^{-5} M) of **$G3NH_3^+$** and **2** in CH_2Cl_2 (bottom).

The ES-MS analysis of a 2:1 mixture of **$G3NH_3^+$** and **2** was carried out under similar conditions (V_c = 350 V, Figure 5). The spectrum thus obtained was largely dominated by the singly charged ion peak corresponding to nonassociated **$G3NH_3^+$**. Whereas a very minor signal ascribed to the 1:1 supramolecular complex [**$G3NH_3^+$·2**] was observed at m/z = 8831.4, the ion peak corresponding to [(**$G3NH_3^+$**)$_2$·**2**] was not detected under these experimental conditions. Owing to the high molecular weight of the dicationic moiety of [(**$G3NH_3^+$**)$_2$·**2**] (16656.65), its response factor must be very low and its detection would require higher V_c values. Unfortunately, the ammonium–crown ether complexes are not stable enough to withstand such harsh conditions.

Absorption and emission binding studies: To quantify the interactions between the crown ether hosts and the C_{60}-ammonium guests, the complexation between the fullerodendrons **$G(1–3)NH_3^+$** and both **1** and **2** was investigated in CH_2Cl_2 by means of UV-visible absorption binding studies. For comparison purposes, binding studies were also performed with a reference unsubstituted benzylammonium guest (**$G0NH_3^+$**). As a typical example, the titration of crown ether **2** with **$G2NH_3^+$** is depicted in Figure 6.

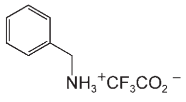

$G0NH_3^+$

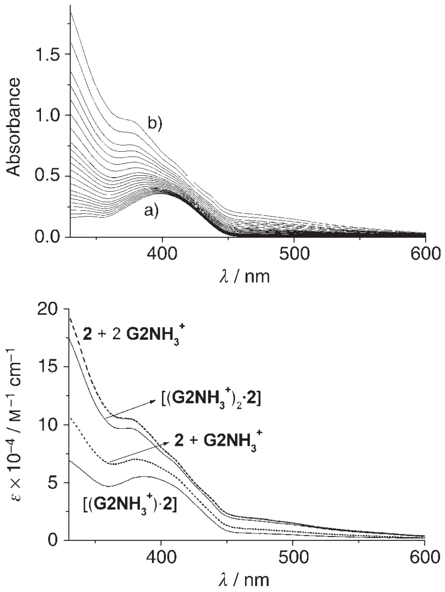

Figure 6. Top: UV/Vis absorption spectrophotometric titration of **2** with **$G2NH_3^+$**; l = 2 cm; a) [**2**]$_{tot}$ = 4.01×10^{-6} M; b) [**$G2NH_3^+$**]$_{tot}$/[**2**]$_{tot}$ = 2.8; solvent: CH_2Cl_2; T = 25.0 ± 0.2 °C. Bottom: Absorption electronic spectra of [**$G2NH_3^+$·2**] and [(**$G2NH_3^+$**)$_2$·**2**] (——) compared with the spectra obtained by summing the spectra of the individual components (-----) showing the weak complexation-induced absorption changes; solvent: CH_2Cl_2; T = 25.0 ± 0.2 °C.

The spectral changes occurring upon successive addition of **$G(0–3)NH_3^+$** to a solution of **1** or **2** in CH_2Cl_2 were monitored. The binding constants deduced from the resulting data are summarized in Table 1. In the case of the ditopic crown ether receptor **2**, the processing of the spectrophotometric data led to the characterization of both 1:1 and 2:1

Table 1. Stability constants determined by the UV/Vis and luminescence binding studies.[a]

	1	**2**		
	$\log K_1$	$\log K_1$	$\log K_2$	K_2/K_1
$G0NH_3^+$	4.6(3)[b]	4.5(9)[b]	3.4(1.8)[b]	0.08(0.12)
	nd	nd	nd	
$G1NH_3^+$	5.9(8)[b,d]	5.6(8)[b,d]	6.5(2)[b,d]	
	4.80(4)[c,d]	5.0(1)[c,d]	5.6(1)[c,d]	4.0(1.2)
$G2NH_3^+$	5.5(3)[b]	5.8(6)[b]	6.7(8)[b]	
	5.15(2)[c]	5.33(1)[c]	6.3(1)[c]	9(3)
$G3NH_3^+$	5.8(7)[b]	nd	$\log\beta_2 = 12.6(9)$[b]	
	5.36(2)[c]	5.28(7)[c]	6.48(7)[c]	16(4)

[a] All the measurements have been carried out in CH_2Cl_2 at 25 ± 0.2 °C except for **$G0NH_3^+$** for which a ternary solvent was used (CH_2Cl_2/CH_3CN/H_2O 50:48:2). The errors correspond to standard deviations given as 3σ; nd = not determined. [b] Determined by UV/Vis absorption titration. [c] Determined by indirect luminescence titration. [d] From ref. [7].

supramolecular edifices and the two successive binding constants defined by the equilibria shown in Equations (1) and (2) were determined, while a single species was observed with the monotopic receptor **1** [Eq. (3)].

$$\mathbf{G(0-3)NH_3^+} + \mathbf{2} \overset{K_1}{\rightleftharpoons} [\mathbf{G(0-3)NH_3^+} \cdot \mathbf{2}] \tag{1}$$

$$\text{in which } K_1 = \frac{[\mathbf{G(0-3)NH_3^+} \cdot \mathbf{2}]}{[\mathbf{2}][\mathbf{G(0-3)NH_3^+}]}$$

$$\mathbf{G(0-3)NH_3^+} + [\mathbf{G(0-3)NH_3^+} \cdot \mathbf{2}] \overset{K_2}{\rightleftharpoons} [(\mathbf{G(0-3)NH_3^+})_2 \cdot \mathbf{2}] \tag{2}$$

$$\text{in which } K_2 = \frac{[(\mathbf{G(0-3)NH_3^+})_2 \cdot \mathbf{2}]}{[\mathbf{G(0-3)NH_3^+} \cdot \mathbf{2}][\mathbf{G(0-3)NH_3^+}]}$$

$$\mathbf{G(0-3)NH_3^+} + \mathbf{1} \overset{K_1}{\rightleftharpoons} [\mathbf{G(0-3)NH_3^+} \cdot \mathbf{1}] \tag{3}$$

$$\text{in which } K_1 = \frac{[\mathbf{G(0-3)NH_3^+} \cdot \mathbf{1}]}{[\mathbf{1}][\mathbf{G(0-3)NH_3^+}]}$$

Owing to the rather weak complexation-induced absorption changes upon addition of the ammonium guests to the solutions of **1** or **2** (Figure 6), the binding constants were obtained with high errors. This prompted us to further investigate the binding of the fullerodendrons to **1** and **2** by means of luminescence studies. Indeed, the strong emission of the π-conjugated system of **1** ($\lambda_{em}^{max} = 440$ nm, $\Phi_{fluo} = 0.72 \pm 0.07$) or **2** ($\lambda_{em}^{max} = 450$ nm, $\varphi_{fluo} = 0.65 \pm 0.06$) is dramatically quenched upon binding of the fullerene-containing dendritic ammonium derivatives $\mathbf{G2NH_3^+}$ and $\mathbf{G3NH_3^+}$. This is illustrated in Figure 7, which shows the emission spectra recorded from solutions of **2** in CH_2Cl_2 before and after addition of $\mathbf{G3NH_3^+}$. A large decrease in the intensity of the characteristic OPV emission was observed when the fullerene ammonium salt $\mathbf{G3NH_3^+}$ was added to the solution of **2**. This decrease can be attributed, at least in part, to the absorption of a fraction of the incoming light by the fullerene moieties of $\mathbf{G3NH_3^+}$, the reabsorption of the OPV luminescence by $\mathbf{G3NH_3^+}$ and intermolecular (collisional) quenching.[7,13] However, experiments carried out in parallel with mixtures of **2** and **G3NHBoc**, which are not able to form a supramolecular complex, show that the decrease in the luminescence intensity mainly originates from an intramolecular photoinduced process in the supramolecular complexes $[\mathbf{G3NH_3^+{\cdot}2}]$ and $[(\mathbf{G3NH_3^+})_2\mathbf{{\cdot}2}]$. Further evidence for an intramolecular quenching of the OPV excited state by the fullerene moiety was obtained by addition of 1,4-diazabicyclo[2.2.2]octane (DABCO) to the mixture of $\mathbf{G3NH_3^+}$ and **2** in CH_2Cl_2. The fluorescence intensity of the resulting solution was found to be similar to that of the reference solution containing **G3NHBoc** and **2**. In other words, treatment with a base deprotonates the ammonium moiety of $\mathbf{G3NH_3^+}$ and thereby disrupts the noncovalent bonding interactions that brought the components together. The efficient photoinduced process at the origin of the intramolecular quenching of the photoexcited OPV within the supramolecular complexes $[\mathbf{G3NH_3^+{\cdot}2}]$ and $[(\mathbf{G3NH_3^+})_2\mathbf{{\cdot}2}]$ can be ascribed to either energy transfer or electron transfer to the fullerene acceptor. Steady-state measurements are not sufficient to determine the nature of the quenching because the residual OPV emission overlaps the much weaker fullerene emission, thus prohibiting clean excitation spectra. However, based on the photophysical studies of related covalent fullerene–OPV conjugates,[14] the most probable deactivation pathway is photoinduced energy transfer.

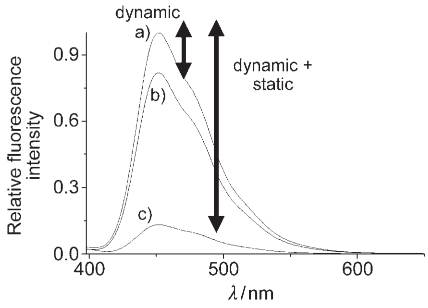

Figure 7. Intramolecular (static) and intermolecular (dynamic: collisional and reabsorption) interactions between $\mathbf{G3NH_3^+}$ and **2**. Solvent: CH_2Cl_2; $T = 25.0 \pm 0.2$ °C; $\lambda_{ex} = 398$ nm; emission and excitation slit widths 15 and 20 nm, respectively; 1% attenuator; a) $[\mathbf{2}]_{tot} = 9.44 \times 10^{-7}$ M; b) $[\mathbf{G3NH_3^+}]_{tot}/[\mathbf{2}]_{tot} = 2.02$ (+0.02% DABCO (by weight)); c) $[\mathbf{G3NH_3^+}]_{tot}/[\mathbf{2}]_{tot} = 2.02$.

The efficient intramolecular photoinduced process in the supramolecular assemblies obtained from $\mathbf{G(2{-}3)NH_3^+}$ and **1** or **2** allowed us to easily determine the association constant by means of luminescence titrations. The experimental conditions are similar to those already used to determine the K values of both **1** and **2** with $\mathbf{G1NH_3^+}$.[7] Because both intramolecular and intermolecular quenching (collisional and/or reabsorption) processes occur upon addition of $\mathbf{G(2{-}3)NH_3^+}$ to solutions of **1** or **2** in CH_2Cl_2, all the luminescence binding studies were carried out with or without DABCO in order to have a suitable reference at all times.[13] As a comparison with a reference solution is always carried out, the intermolecular quenching processes can be ignored and the difference in emission intensity between the two solutions only accounts for the intramolecular quenching of the OPV excited state by a fullerene moiety in the supramolecular complexes. In order to determine the binding constants, the fluorescence titration data were analyzed according to the following modified Stern–Volmer equations[7] [Eq. (4) for **1** and Eq. (5) for **2**]:

$$\frac{F^0}{F} = (1 + K_{SV}[\mathbf{G(2-3)NH_3^+}])(1 + K_1[\mathbf{G(2-3)NH_3^+}]) \tag{4}$$

$$\frac{F^0}{F} = (1 + K_{SV}[\mathbf{G(2-3)NH_3^+}])(1 + K_1[\mathbf{G(2-3)NH_3^+}] + K_1K_2[\mathbf{G(2-3)NH_3^+}]^2) \tag{5}$$

in which F^0 is the normalized fluorescence intensity of the OPV derivative (**1** or **2**) in the absence of $\mathbf{G(2{-}3)NH_3^+}$, F the fluorescence intensity of the OPV derivative (**1** or **2**) in the presence of **G(2–3)NH$_3$$^+$**, [**G(2–3)NH$_3$$^+$**] the molar concentration of fullerene derivative **G(2–3)NH$_3$$^+$**, and K_{SV} the pseudo Stern–Volmer constant. The K_{SV} values for both **G2NH$_3$$^+$** and **G3NH$_3$$^+$** were determined from luminescence titrations carried out under the same experimental conditions with **G2NHBoc** and **G3NHBoc**, respectively, according to the classical Stern–Volmer treatment.[15] As a typical example, the luminescence titration of **2** with **G3NH$_3$$^+$** and the fitting of the experimental data according to Equation (5) are shown in Figure 8. The association constants determined from the emission binding studies of both **1** and **2** with **G(1–3)NH$_3$$^+$** are summarized in Table 1. The log$K$ values determined from indirect luminescence titration are lower by approximately 0.6 to one order of magnitude with respect to those obtained from the spectrophotometric titrations (Table 1). These differences could originate from the high errors of the log$K$ values deduced from the UV-visible binding studies.

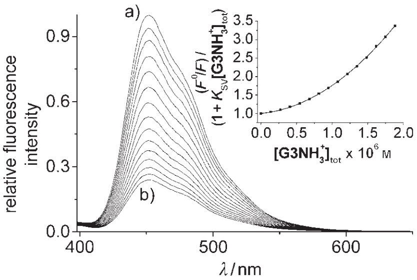

Figure 8. Luminescence titration ($F^0/(F\times(1+K_{SV}[\mathbf{G3NH_3^+}]))$) of **2** by **G3NH$_3$$^+$**. Solvent: CH_2Cl_2; $T = 25.0 \pm 0.2$ °C; $\lambda_{ex} = 398$ nm; $\lambda_{ana} = 450$ nm; emission and excitation slit widths 15 and 20 nm, respectively; 1% attenuator; a) $[\mathbf{2}]_{tot} = 9.44\times10^{-7}$ M; b) $[\mathbf{G3NH_3^+}]_{tot}/[\mathbf{2}]_{tot} = 2.02$. The curves correspond to the nonlinear least-squares fit of experimental data according to Equation (5).

Several key points can be deduced from the results reported in Table 1. Interestingly, a strong stabilization of approximately one to two orders of magnitude is observed, when the logK_1 values (**1** and **2**) are compared with those generally reported in the literature for complexes formed between crown ether derivatives and various ammonium cations.[4b,11a,16] The logK_1 values for the binding of fullerodendrons **G(1–3)NH$_3$$^+$** to both **1** and **2** are also approximately one order of magnitude higher than that of the simple benzylammonium guest **G0NH$_3$$^+$**. Moreover, it is noteworthy that logK_1 values slightly increase with the size of the branches. The sum of secondary weak intramolecular interactions, such as π–π stacking and hydrophobic interactions within the supramolecular structures, which result from the association of **1** or **2** with **G(1–3)NH$_3$$^+$**, must be at the origin of this stronger coordination.

As far as the 2:1 noncovalent arrays obtained from **2** are concerned, the K_2/K_1 ratios provide a criterion to quantify the interactions between the two identical and independent binding sites.[17] For the binding of **G(1–3)NH$_3$$^+$** to **2**, the K_2/K_1 values summarized in Table 1 are significantly larger than 0.25, which is the value expected for a statistical model,[17] and clearly indicates positive intramolecular interactions in the 2:1 associates [(**G(1–3)NH$_3$$^+$**)$_2$·**2**]. The latest observation may be ascribed to strong intramolecular fullerene–fullerene interactions between the two **G(1–3)NH$_3$$^+$** guests within [(**G(1–3)NH$_3$$^+$**)$_2$·**2**]. This hypothesis is also supported by the absence of any positive interactions for the 2:1 complex obtained from **2** and the ammonium derivative **G0NH$_3$$^+$** that lacks the fullerene subunits for which the K_2/K_1 ratio is approximately 0.08(0.12). Finally, it is also important to highlight that the K_2/K_1 ratio significantly increases as the size of the dendritic branches increases. In other words, the cooperative effect is more and more effective when the number of C_{60} units increases. This positive dendritic effect further confirms that intramolecular fullerene–fullerene interactions must be at the origin of the observed cooperative effect.

Conclusion

Dendritic branches with 1, 2, or 4 peripheral fullerene subunits and an ammonium function at the focal point have been prepared. Their ability to form self-assembled dendritic supramolecular structures with crown ether receptors has been evidenced by ES-MS studies for the first time. Further binding studies were easily carried out in solution owing to the efficient intramolecular quenching of the emission of the crown ether receptors by the C_{60} acceptor within the noncovalent arrays. The presence of the fullerene subunits in the dendritic guests is not only important for their ability to act as energy acceptors in the host–guest assemblies, but they are also at the origin of the positive cooperative effect and increase the stability of the 2:1 complexes obtained from the fullerodendrons and the ditopic receptor. The results reported in this paper show that the size of dendritic building blocks does not constitute a severe limitation for the self-assembly of large dendritic architectures. Furthermore, it appears that the stability of the highest generation supramolecular ensemble is increased owing to the increased number of possible secondary interactions within the self-assembled structure.

Experimental Section

General: All reagents were used as purchased from commercial sources without further purification. Compounds **1**,[11a] **2**,[7] **3**–**4**,[8] **5**,[9] and **G1NH$_3$$^+$**[7] were prepared according to previously reported procedures. UV/Vis spectra were measured on a Hitachi U-3000 spectrophotometer. IR spectra were determined on an ATI Mattson Genesis Series FTIR instrument. NMR spectra were recorded on a Bruker AM300 (300 MHz) with the solvent signal as the reference. Mass spectrometry measurements were carried out on a Bruker BIFLEX^{TM} matrix-assisted laser desorption ionization time-of-flight (MALDI-TOF) mass spectrometer.

Compound G2NHBoc: DCC (164.4 mg, 0.80 mmol) was added to a stirred solution of **3** (300 mg, 0.08 mmol), **5** (94.6 mg, 0.40 mmol), DMAP (9.7 mg, 0.08 mmol), and a catalytic amount of HOBt in CH_2Cl_2 (20 mL) at 0 °C. After 1 h at 0 °C, the mixture was allowed to slowly warm to RT, and then it was stirred for 4 d. The resulting solid was filtered off and the solvent removed under reduced pressure. Column chromatography (silica gel, CH_2Cl_2/0.5 % MeOH) followed by preparative size-exclusion chromatography (Biorad Biobeads SX-1, CH_2Cl_2) yielded **G2NHBoc** as a dark orange glassy product (284 mg, 89 %). ^{1}H NMR (300 MHz, $CDCl_3$): $\delta = 0.89$ (t, $J = 7$ Hz, 24 H), 1.21–1.41 (m, 80 H), 1.43 (s, 9 H), 1.71 (m, 16 H), 3.86 (t, $J = 7$ Hz, 16 H), 4.29 (d, $J = 6$ Hz, 2 H), 4.68 (m, 6 H), 4.92 (brs, 1 H), 5.03 (d, $J = 13$ Hz, 4 H), 5.19 (m, 6 H), 5.27 (m, 8 H), 5.71 (d, $J = 13$ Hz, 4 H), 6.34 (t, $J = 2$ Hz, 4 H), 6.43 (d, $J = 2$ Hz, 8 H), 6.76 (s, 4 H), 6.83 (s, 2 H), 6.98 (s, 1 H), 7.12 (s, 2 H), 7.27 ppm (m, 4 H); ^{13}C NMR (75 MHz, $CDCl_3$): $\delta = 14.3$, 22.8, 26.3, 28.6, 29.4, 29.5, 32.0, 49.2, 65.5, 65.6, 66.5, 67.0, 67.3, 68.3, 68.9, 70.7, 79.7, 101.8, 107.3, 112.7, 114.7, 116.3, 121.5, 127.8, 129.0, 134.3, 134.5, 135.9, 136.2, 136.7, 137.5, 137.5, 137.9, 138.6, 139.8, 140.1, 141.2, 141.3, 142.4, 142.8, 143.3, 143.7, 143.9, 144.1, 144.3, 144.4, 144.7, 145.07, 145.14, 145.3, 145.5, 145.7, 145.9, 146.2, 147.45, 147.55, 147.6, 148.8, 156.0, 157.9, 158.3, 160.5, 162.7, 162.75, 168.4, 168.5 ppm; IR (CH_2Cl_2): $\tilde{\nu} = 1747\ cm^{-1}$ (C=O); UV/Vis (CH_2Cl_2): λ (ε) = 259 (321 220), 318 (98 250), 438 (9820), 705 nm (80 $mol^{-1}dm^3cm^{-1}$); elemental analysis calcd (%) for $C_{267}H_{201}NO_{35}$: C 80.51, H 5.09, N 0.35; found: C 80.44, H 5.02, N 0.23.

Compound G2NH$_3^+$: A solution of **G2NHBoc** (165 mg, 41 μmol) and trifluoroacetic acid (5 mL) in CH_2Cl_2 (10 mL) was stirred for 4 h at RT. The organic phase was diluted with CH_2Cl_2 (50 mL), washed with water (50 mL), dried over $MgSO_4$, and the solvent was removed under reduced pressure. Purification by preparative size-exclusion chromatography (Biorad Biobeads SX-1, CH_2Cl_2) yielded **G2NH$_3^+$** as a dark orange glassy product (130 mg, 79 %). ^{1}H NMR (300 MHz, $CDCl_3$): $\delta = 0.89$ (t, $J = 6$ Hz, 24 H), 1.21–1.41 (m, 80 H), 1.71 (m, 16 H), 3.86 (t, $J = 6$ Hz, 16 H), 4.03 (brs, 2 H), 4.59 (s, 4 H), 4.70 (s, 2 H), 5.05 (d, $J = 13$ Hz, 4 H), 5.15 (m, 6 H), 5.29 (brs, 8 H), 5.70 (d, $J = 13$ Hz, 4 H), 6.34 (t, $J = 2$ Hz, 4 H), 6.47 (d, $J = 2$ Hz, 8 H), 6.71 (s, 2 H), 6.81 (s, 4 H), 6.96 (s, 1 H), 7.09 (m, 4 H), 7.18 ppm (s, 2 H); ^{13}C NMR (75 MHz, $CDCl_3$): $\delta = 14.3$, 22.8, 26.3, 29.4, 29.5, 32.0, 49.2, 65.5, 65.6, 66.7, 67.0, 67.3, 68.1, 68.9, 70.5, 101.8, 107.3, 112.6, 114.7, 116.3, 121.4, 127.8, 129.0, 134.4, 134.5, 135.9, 136.3, 136.7, 137.5, 137.5, 137.9, 138.6, 139.8, 140.1, 141.2, 141.3, 142.4, 142.8, 143.3, 143.7, 143.9, 144.1, 144.3, 144.4, 144.7, 145.1, 145.15, 145.3, 145.5, 145.7, 145.9, 146.2, 147.45, 147.6, 147.65, 148.8, 156.0, 157.9, 158.3, 160.4, 162.7, 162.75, 168.4, 168.7 ppm; IR (CH_2Cl_2): $\tilde{\nu} = 1748\ cm^{-1}$ (C=O); UV/Vis (CH_2Cl_2): λ (ε) = 259 (310 390), 318 (97 100), 438 (9750), 705 nm (70 $mol^{-1}dm^3cm^{-1}$); ES-MS: m/z calcd for $C_{262}H_{194}NO_{33}$: 3884.34 $[M-CF_3COO^-]^+$; found: 3884.

Compound G3NHBoc: DCC (142.2 mg, 0.69 mmol) was added to a stirred solution of **4** (531.0 mg, 69 μmol), **5** (81.8 mg, 0.35 mmol), DMAP (8.4 mg, 69 μmol), and a catalytic amount of HOBt in CH_2Cl_2 (25 mL) at 0 °C. After 1 h, the mixture was allowed to slowly warm to RT, and it was then stirred for 5 d. The resulting solid was filtered off and the solvent removed under reduced pressure. Column chromatography (silica gel, CH_2Cl_2/2 % MeOH) followed by preparative size-exclusion chromatography (Biorad Biobeads SX-1, CH_2Cl_2) yielded **G3NHBoc** as a dark orange glassy product (365 mg, 67 %). ^{1}H NMR (300 MHz, $CDCl_3$, 25 °C): $\delta = 0.89$ (t, $J = 7$ Hz, 48 H), 1.20–1.44 (m, 160 H), 1.46 (s, 9 H), 1.71 (m, 32 H), 3.82 (t, $J = 7$ Hz, 32 H), 4.30 (d, $J = 6$ Hz, 2 H), 4.60 (s, 2 H), 4.66 (m, 12 H), 5.04 (m, 9 H), 5.18 (m, 14 H), 5.28 (m, 16 H), 5.70 (d, $J = 13$ Hz, 8 H), 6.34 (t, $J = 2$ Hz, 8 H), 6.42 (d, $J = 2$ Hz, 16 H), 6.75 (s, 8 H), 6.81 (s, 2 H), 6.84 (m, 5 H), 6.98 (s, 2 H), 7.12 (s, 4 H), 7.24 ppm (m, 4 H); ^{13}C NMR (75 MHz, $CDCl_3$, 25 °C): $\delta = 14.3$, 22.9, 26.3, 28.6, 29.5, 29.6, 32.1, 49.2, 65.46, 65.47, 65.6, 66.6, 67.0, 67.3, 68.3, 68.9, 70.8, 79.7, 101.9, 107.4, 112.7, 114.7, 114.8, 116.3, 121.5, 121.6, 127.9, 129.1, 134.3, 134.6, 136.0, 136.3, 136.8, 137.5, 137.6, 138.0, 138.7, 139.9, 140.2, 141.25, 141.3, 142.5, 142.9, 143.4, 143.8, 143.9, 144.1, 144.4, 144.5, 144.6, 144.8, 145.1, 145.2, 145.4, 145.5, 145.8, 145.9, 146.3, 147.5, 147.7, 148.8, 158.0, 158.3, 160.6, 162.7, 162.8, 168.5 ppm; IR (CH_2Cl_2): $\tilde{\nu} = 1747\ cm^{-1}$ (C=O); UV/Vis (CH_2Cl_2): λ (ε) = 260 (502 860), 318 (195 200), 438 (17 830), 705 nm (160 $mol^{-1}dm^3cm^{-1}$); elemental analysis calcd (%) for $C_{531}H_{393}NO_{71}$: C 80.49, H 5.00, N 0.18; found: C 80.36, H 4.99, N 0.15.

Compound G3NH$_3^+$: A solution of **G3NHBoc** (224 mg, 28 μmol) and trifluoroacetic acid (5 mL) in CH_2Cl_2 (15 mL) was stirred for 5 h at RT. The organic phase was diluted with CH_2Cl_2 (50 mL), washed with water (50 mL), dried over $MgSO_4$, and the solvent was removed under reduced pressure. Purification by preparative size-exclusion chromatography yielded **G3NH$_3^+$** as a dark orange glassy product (140.6 mg, 63 %). ^{1}H NMR (300 MHz, $CDCl_3$, 25 °C): $\delta = 0.89$ (t, $J = 7$ Hz, 48 H), 1.20–1.44 (m, 160 H), 1.71 (m, 32 H), 3.82 (t, $J = 7$ Hz, 32 H), 4.00 (brs, 2 H), 4.58 (s, 2 H), 4.66 (m, 12 H), 5.10 (m, 22 H), 5.28 (m, 16 H), 5.68 (d, $J = 13$ Hz, 8 H), 6.32 (t, $J = 2$ Hz, 8 H), 6.44 (d, $J = 2$ Hz, 16 H), 6.65 (s, 2 H), 6.65 (m, 8 H), 6.78 (m, 5 H), 6.92 (s, 2 H), 7.12 ppm (m, 8 H); ^{13}C NMR (75 MHz, $CDCl_3$, 25 °C): $\delta = 14.3$, 22.9, 26.3, 29.5, 29.6, 32.1, 49.2, 65.46, 65.47, 65.6, 66.8, 67.0, 67.5, 68.3, 69.0, 70.6, 101.9, 107.4, 112.7, 114.6, 114.8, 116.3, 121.5, 121.7, 127.9, 129.1, 134.3, 134.6, 136.0, 136.4, 136.8, 137.5, 137.6, 138.0, 138.7, 139.9, 140.2, 141.25, 141.3, 142.7, 142.9, 143.4, 143.8, 143.9, 144.1, 144.4, 144.5, 144.6, 144.8, 145.1, 145.2, 145.4, 145.5, 145.8, 145.9, 146.3, 147.5, 147.8, 148.8, 158.0, 158.4, 160.6, 162.6, 162.8, 168.7 ppm; IR (CH_2Cl_2): $\tilde{\nu} = 1748\ cm^{-1}$ (C=O); UV/Vis (CH_2Cl_2): λ (ε) = 260 (504 270), 318 (192 480), 438 (16 340), 705 nm (150 $mol^{-1}dm^3cm^{-1}$); MALDI-TOF-MS: m/z calcd for $C_{526}H_{386}NO_{69}$: 7824.68 $[M-CF_3COO^-]^+$; found: 7825.

ES-MS: High-resolution ES mass spectra were recorded in the positive mode on a time-of-flight mass spectrometer (microTof, Bruker Daltonics, Bremen, Germany). The instrument was calibrated with a solution of CsI, 1 $mg\,mL^{-1}$, in water/isopropanol 50:50 (v/v). CsI clusters of type $[(CsI)_nCs]^+$ or $[(CsI)_nCs_2]^{2+}$ generate ions with an m/z of up to ≈16 000. The ESI source was heated to 100 °C. Sample solutions were introduced into the mass spectrometer source with a syringe pump (Cole Parmer, Vernon Hills, Illinois, USA) with a flow rate of 5 $\mu L\,min^{-1}$. Scanning was performed on a m/z range from 100 to 16 000, data were averaged for 1 min and then smoothed by means of the Gaussian algorithm. To make sure that the species detected by ES-MS faithfully reflect the species present in solution, instrument parameters were systematically varied, for example, sample cone voltage V_c.

UV/Vis and fluorescence titrations: Binding studies were carried out as already described in detail in a previous paper.[7]

Acknowledgements

This work was supported by the CNRS, a doctoral fellowship from the French Ministry of Research to A.T., a doctoral fellowship from the CNRS and the Région Alsace to F.C., a doctoral fellowship from the European Postgraduate School (GRK532) to H.H. and a post-doctoral fellowship from the Deutscher Akademischer Austausch Dienst (DAAD) to U.H.

---

[1] a) G. R. Newkome, C. N. Moorefield, F. Vögtle, *Dendrimers and Dendrons: Concepts, Syntheses, Applications*, VCH, Weinheim, **2001**; b) *Dendrimers and other Dendritic Polymers* (Eds.: J. M. J. Fréchet, D. A. Tomalia), Wiley, Chichester, **2001**.

[2] For reviews on supramolecular dendrimer chemistry, see: a) F. Zeng, S. C. Zimmerman, *Chem. Rev.* **1997**, *97*, 1681–1712; b) D. K. Smith, F. Diederich, *Chem. Eur. J.* **1998**, *4*, 1353–1361; c) G. C. Newkome, E. He, C. N. Moorefield, *Chem. Rev.* **1999**, *99*, 1689–1746; d) A. E. Kaifer, *Acc. Chem. Res.* **1999**, *32*, 62–71; e) D. K. Smith, A. R. Hirst, C. S. Love, J. G. Hardy, S. V. Brignell, B. Huang, *Prog. Polym. Sci.* **2005**, *30*, 220–293.

[3] For selected examples, see: a) S. C. Zimmerman, F. Zeng, D. E. C. Reichert, S. V. Kolotuchin, *Science* **1996**, *271*, 1095–1098; b) P. Thiyagarajan, F. Zeng, C. Y. Ku, S. C. Zimmerman *J. Mater. Chem.* **1997**, *7*, 1221–1226; c) F. Zeng, S. C. Zimmerman, S. V. Kolotuchin, D. E. C. Reichert, Y. G. Ma, *Tetrahedron* **2002**, *58*, 825–843; d) E. R. Gillies, J. M. J. Fréchet, *J. Org. Chem.* **2004**, *69*, 46–53.

[4] For selected examples, see: a) Y. Wang, F. W. Zeng, S. C. Zimmerman, *Tetrahedron Lett.* **1997**, *38*, 5459–5462; b) G. M. Dykes, D. K. Smith, G. J. Seeley, *Angew. Chem.* **2002**, *114*, 3388–3391; *Angew. Chem. Int. Ed.* **2002**, *41*, 3254–3257; c) B. Kenda, F. Diederich, *Angew. Chem.* **1998**, *110*, 3357–3361; *Angew. Chem. Int. Ed.* **1998**,

37, 3154–3158; d) N. Yamaguchi, L. M. Hamilton, H. W. Gibson, *Angew. Chem.* **1998**, *110*, 3463–3466; *Angew. Chem. Int. Ed.* **1998**, *37*, 3275–3279; e) H. W. Gibson, N. Yamaguchi, L. Hamilton, J. W. Jones, *J. Am. Chem. Soc.* **2002**, *124*, 4653–4665; f) M.-C. Daniel, F. Ba, J. R. Aranzaes, D. Astruc, *Inorg. Chem.* **2004**, *43*, 8649–8657.

[5] For selected examples, see: a) G. R. Newkome, F. Cardullo, E. C. Constable, C. N. Moorefield, A. M. W. Cargill Thompson, *J. Chem. Soc., Chem. Commun.* **1993**, 925–926; b) G. R. Newkome, K. S. Yoo, S.-H. Hwang, C. N. Moorefield, *Tetrahedron* **2003**, *59*, 3955–3964; c) G. R. Newkome, K. S. Yoo, H. J. Kim, C. N. Moorefield, *Chem. Eur. J.* **2003**, *9*, 3367–3374; d) A. W. Kleij, R. van de Coevering, R. J. M. Klein Gebbink, A. M. Noordman, A. L. Spek, G. van Koten, *Chem. Eur. J.* **2001**, *7*, 181–192.

[6] a) R. van de Coevering, R. Kreiter, F. Cardinali, G. van Koten, J.-F. Nierengarten, R. J. M. Klein Gebbink, *Tetrahedron Lett.* **2005**, *46*, 3353–3356; b) U. Hahn, J. J. González, E. Huerta, M. Segura, J.-F. Eckert, F. Cardinali, J. de Mendoza, J.-F. Nierengarten, *Chem. Eur. J.* **2005**, *11*, 6666–6672.

[7] M. Elhabiri, A. Trabolsi, F. Cardinali, U. Hahn, A.-M. Albrecht-Gary, J.-F. Nierengarten, *Chem. Eur. J.* **2005**, *11*, 4793–4798.

[8] J.-F. Nierengarten, D. Felder, J.-F. Nicoud, *Tetrahedron Lett.* **1999**, *40*, 269–272.

[9] A. Zistler, S. Kock, A. D. Schlüter, *J. Chem. Soc. Perkin Trans. 1* **1999**, 501–508.

[10] C. A. Schalley, *Int. J. Mass Spectrom.* **2000**, *194*, 11–39.

[11] a) M. Gutiérrez-Nava, H. Nierengarten, P. Masson, A. Van Dorsselaer, J.-F. Nierengarten, *Tetrahedron Lett.* **2003**, *44*, 3043–3046; b) U. Hahn, M. Elhabiri, A. Trabolsi, H. Herschbach, E. Leize, A. Van Dorsselaer, A.-M. Albrecht-Gary, J.-F. Nierengarten, *Angew. Chem.* **2005**, *117*, 5472–5475; *Angew. Chem. Int. Ed.* **2005**, *44*, 5338–5341.

[12] M. Gutiérrez-Nava, G. Accorsi, P. Masson, N. Armaroli, J.-F. Nierengarten, *Chem. Eur. J.* **2004**, *10*, 5076–5086.

[13] N. Armaroli, F. Diederich, L. Echegoyen, T. Habicher, L. Flamigni, G. Marconi, J.-F. Nierengarten, *New J. Chem.* **1999**, *23*, 77–83.

[14] a) N. Armaroli, F. Barigelletti, P. Ceroni, J.-F. Eckert, J.-F. Nicoud, J.-F. Nierengarten, *Chem. Commun.* **2000**, 599–600; b) J.-F. Eckert, J.-F. Nicoud, J.-F. Nierengarten, S.-G. Liu, L. Echegoyen, F. Barigelletti, N. Armaroli, L. Ouali, V. Krasnikov, G. Hadziioannou, *J. Am. Chem. Soc.* **2000**, *122*, 7467–7479; c) E. Peeters, P. A. van Hal, J. Knol, C. J. Brabec, N. S. Sariciftci, J. C. Hummelen, R. A. J. Janssen, *J. Phys. Chem. B* **2000**, *104*, 10174–10190; d) J. L. Segura, R. Gomez, N. Martín, D. M. Guldi, *Chem. Commun.* **2000**, 701–702; e) G. Accorsi, N. Armaroli, J.-F. Eckert, J.-F. Nierengarten, *Tetrahedron Lett.* **2002**, *43*, 65–68; f) D. M. Guldi, A. Swartz, C. Luo, R. Gomez, J. L. Segura, N. Martín, *J. Am. Chem. Soc.* **2002**, *124*, 10875–10886; g) For a review on fullerene–(π-conjugated oligomer) dyads, see: J. L. Segura, N. Martín, D. M. Guldi, *Chem. Soc. Rev.* **2005**, *34*, 31–47.

[15] It is important to note that the K_{SV} values thus obtained do not correspond to the Stern–Volmer constant of a collisional intermolecular quenching process because a large part of the decrease in emission intensity is actually caused by the reabsorption of the OPV luminescence by the fullerene derivative, see ref. [7].

[16] a) R. M. Izatt, K. Pawlak, J. S. Bradshaw, R. L. Bruening, *Chem. Rev.* **1991**, *91*, 1721–2085; b) H. R. Pouretedal, M. Shamsipur, *J. Chem. Eng. Data* **1998**, *43*, 742–744; c) G. M. Dykes, D. K. Smith, *Tetrahedron* **2003**, *59*, 3999–4009.

[17] a) B. Perlmutter-Hayman, *Acc. Chem. Res.* **1986**, *19*, 90–96; b) G. Ercolani, *J. Am. Chem. Soc.* **2003**, *125*, 16097–16103.

Received: October 8, 2005